Journal of Alloys and Compounds 522 (2012) 39–45

Contents lists available at SciVerse ScienceDirect

Journal of Alloys and Compounds

journal homepage: www.elsevier.com/locate/jallcom

Comparative study of nano copper aluminate spinel prepared by sol–gel and modified sol–gel techniques: Structural, electrical, optical and catalytic studies

R. Thinesh Kumar[a], P. Suresh[a], N. Clament Sagaya Selvam[a], L. John Kennedy[b,*], J. Judith Vijaya[a,*]

[a] Catalysis and Nanomaterials Research Laboratory, Department of Chemistry, Loyola College, Chennai 34, India
[b] Materials Division, School of Advanced Sciences, VIT-University, Chennai Campus, Chennai 48, India

ARTICLE INFO

Article history:
Received 29 August 2011
Received in revised form
31 December 2011
Accepted 12 January 2012
Available online 28 January 2012

Keywords:
Sol–gel process
X-ray diffraction
Thermoelectric
Electron microscopy
Oxidation

ABSTRACT

The effect of ethylenediamine addition in the sol–gel method for the preparation of nano $CuAl_2O_4$ spinel for the enhancement in their structural, electrical, optical and catalytic properties was investigated. The samples were prepared by two different methods: sol–gel and modified sol–gel technique using ethylenediamine. X-ray diffraction (XRD), Fourier transform infrared spectra (FT-IR), scanning electron microscopy (SEM), high resolution-transmission electron microscopy (HR-TEM), energy dispersive X-ray analysis (EDX), nitrogen adsorption/desorption isotherms, temperature dependent conductance measurements, thermoelectric power (TEP) measurements and UV–visible diffuse reflectance (UV–vis-DRS) spectra were used to characterize the samples prepared. $CuAl_2O_4$ prepared by modified sol–gel technique was found to possess a higher surface area, lower crystallite size, lower activation energy and high porosity than the one prepared by sol–gel method which in turn lead to the improved performance of it towards the selective oxidation of benzyl alcohol to benzaldehyde. Effect of solvent on the catalytic oxidation of benzyl alcohol by the nano $CuAl_2O_4$ prepared by modified sol–gel technique was also investigated.

1. Introduction

In general, aluminate spinels show high thermal stability, high mechanical resistance, hydrophobicity and low surface acidity [1,2]. These properties make them interesting materials as catalysts and carriers for active metals to replace current technology. Copper aluminate spinel is known to be active in the degradation of some organic compounds, and is commonly prepared by high temperature calcination of mixed aluminum and copper oxides [3,4], or is the product of impregnating a porous alumina having a high surface area with a solution of copper compound [5]. However, to attain complete reaction, a temperature of above 1500 °C has to be maintained for several days. Recently, MAl_2O_4 (M = Cu, Zn, Mg, Ni and Li) has been prepared by the following methods: co-precipitation [6], hydrothermal synthesis [7] and sol–gel methods [8]. The disadvantages of solid-state routes, such as inhomogeneity, lack of stoichiometry control, high temperature and low surface area, are improved when the material is synthesized utilizing a solution-based method. The high surface area $CuAl_2O_4$ along with small particle sizes is of prime importance for many industrial applications. Hence, the preparation of nanosized copper aluminate particles will be worthwhile to study.

Compared with other techniques, the sol–gel method is a useful and attractive technique for the preparation of aluminate spinels because of its advantage of producing pure and ultrafine powders at low temperatures. A modified sol–gel method for preparing the metal oxides is Pechini method which involves combining a metal precursor with water, citric acid and ethylene glycol [9]. In our present study, we have used the modified sol–gel method with water, citric acid and ethylenediamine along with the metal precursors and compared the powders obtained with the ones obtained by the sol–gel method in order to study the changes in their structural, electrical, optical and catalytic properties by X-ray diffraction (XRD), FT-IR, scanning electron microscopy (SEM), high resolution transmission electron microscopy (HR-TEM), energy dispersive X-ray analysis, nitrogen adsorption–desorption isotherms at 77 K, temperature dependent conductance measurements, thermoelectric power (TEP) measurements, UV–visible diffuse reflectance (UV–vis-DRS) spectra and the products formed by the catalytic oxidation of alcohols were characterized by gas chromatography (GC). Although the literature on the usage of urea, ammonia and ethylene glycol along with the gelling agent citric acid is available [10–12], the literature on the usage of ethylenediamine is scarce. Up to our knowledge there are no reports on the usage of nano copper aluminate spinels prepared by sol–gel or modified sol–gel technique for the catalytic oxidation of alcohols. Hence in the present study, the role of ethylenediamine in enhancing the structural, electrical, optical and catalytic properties of copper aluminate is highlighted and the mechanism for the same is

* Corresponding authors. Tel.: +91 44 28178200; fax: +91 44 28175566.
E-mail addresses: jklsac14@yahoo.co.in (L.J. Kennedy), jjvijayaloyola@yahoo.co.in (J.J. Vijaya).

0925-8388/$ – see front matter © 2012 Elsevier B.V. All rights reserved.
doi:10.1016/j.jallcom.2012.01.064

proposed. Ethylenediamine has always been a good candidate ligand because of its strong alkaliscence, weak polarity, reducibility, strong coordination interaction with metal ions and low boiling point. Vijaya et al. [13,14] have already reported the preparation of nano copper aluminate by sol–gel method and its application as sensors but in the present study, we focused on the role of ethylenediamine in the preparation procedure and how it enhances the structural, electrical, optical and catalytic properties of copper aluminate spinels. Benzyl alcohol oxidation activity tests were carried out to study the influence of preparation method on the catalytic activity of the nano $CuAl_2O_4$ samples. The best activity and selectivity towards catalytic oxidation were observed from the one prepared by modified sol–gel technique.

2. Experimental

All chemicals were of analytical grade and used without any further purification.

2.1. Preparation of copper aluminate by sol–gel method (sample A)

Calculated amounts of copper nitrate and aluminum nitrate were dissolved in double distilled water and thereafter citric acid was added as a gelling agent. The resulting solution was stirred at room temperature for half an hour until a clear transparent solution was obtained. This clear solution was kept for gellation at 5 °C for 12 h and the gel was then dried at 110 °C, followed by calcination at 600 °C for 5 h. The powders were then sintered at 900 °C at a heating rate of 5 °C/min for 5 h in air atmosphere.

2.2. Preparation of copper aluminate by modified sol–gel method (sample B)

Calculated amounts of copper nitrate and aluminum nitrate were dissolved in double distilled water and then citric acid was added as a gelling agent. The resulting solution was stirred at room temperature for half an hour until a clear transparent solution was obtained and the pH was adjusted to 10 by adding ethylene diamine. The resultant solution was heated at 100 °C with constant stirring for an hour and the powders obtained were sintered at 900 °C at a heating rate of 5 °C/min for 5 h in air atmosphere.

2.3. Characterization of samples A and B

Structural characterization of the samples was performed using a Philips X'pert diffractometer for 2θ values ranging from 10 to 80° using CuK_α radiation at $\lambda = 0.154$ nm. A Perkin Elmer infrared spectrophotometer (SPECTRUM RX 1) was used for the determination of the surface functional groups. The surface morphology of the samples was determined by a Leo-Jeol scanning electron microscope at desired magnification. HR-TEM images along with energy dispersive X-ray analysis (EDX) were recorded using a Jeol-Jem 3010 high resolution transmission electron microscope to determine the particle size and elemental analysis of the samples. The surface area and pore size distribution were estimated from the nitrogen adsorption–desorption isotherm using liquid nitrogen at 77 K. Such isotherms were obtained using an automatic adsorption instrument (Quantachrome Corp. Nova-1000 gas sorption analyzer). Prior to the measurement, the samples were degassed at 150 °C for overnight. The surface area of the samples was calculated using BET equation [15], which is the most widely used method for determining the specific surface area (m^2/g). To that aim, the area of the nitrogen molecule is assumed to be 0.162 nm^2. The pore size distribution was determined using the BJH method. In addition, the *t*-plot method [16] was applied to calculate the micropore volume and external surface area. The total pore volume was estimated as the liquid volume of the adsorbate adsorbed at a relative pressure of 0.99. The optical studies of the samples were recorded using CARY 100 UV–visible spectrophotometer.

Electrical conductance was studied by making the samples in pellet form employing a pressure of about 1 GPa at room temperature. The studies were measured from 393 to 573 K by two-probe method. The pellets were well polished, and the two surfaces of each pellet were coated with silver paste and ensured for the Ohmic contacts. The samples were electrically connected to a dc power supply and a Keithley 614 digital electrometer in series. The activation energy of the samples was calculated by using Arrhenius expression

$$I = I_o \exp^{-E_a/kT}$$

where I is the current, E_a is the activation energy, k is the Boltzmann constant and T is the temperature.

The thermopower or Seebeck coefficient of a material is a measure of the magnitude of an induced thermoelectric voltage in response to a temperature difference across that material. The p- or n-type semiconductivity of the composites was confirmed by measuring the thermoelectric force of the composites. The thermoelectric or the Seebeck coefficient (θ) of the composites was calculated using the formula, $\theta = \Delta E/\Delta T$.

$$\theta = \frac{\Delta E}{\Delta T}$$

where ΔE is the thermo emf produced across the sample due to the temperature difference ΔT [17].

2.4. Catalytic test

The oxidation of benzyl alcohol was carried out in a batch reactor operated under atmospheric conditions. 10 mmol of oxidant (H_2O_2) was added along with the catalyst and the contents were heated at 80 °C using different solvents like n-hexane, chlorobenzene and acetonitrile for 10 h in a three necked round bottom flask equipped with a reflux condenser and thermometer.

The oxidized products after the catalytic reaction are collected and studied using Agilent GC spectrometer. The column used for the study was DB wax column (capillary column) of length 30 mm and helium was used as the carrier gas.

3. Results and discussion

3.1. X-ray diffraction analysis

The structural phases of samples A and B were determined by X-ray diffraction pattern. Fig. 1a displays the XRD pattern of the sol–gel synthesized sample and Fig. 1b displays the XRD pattern of sample synthesized by modified sol–gel method using ethylenediamine as precipitating agent/complexing agent. Both samples A and B, showed diffraction peaks at 2θ values of 31.18, 36.91, 44.90, 55.73, 59.44 and 65.45° corresponding to the [2 2 0], [3 1 1], [4 0 0], [4 2 2], [5 1 1] and [4 4 0] planes respectively. These planes are associated with the spinel type $CuAl_2O_4$ with cubic structure matching with the JCPDS card no. 33-0448.

Further observation revealed that the sample A and sample B have sharp peaks, indicating good crystallinity, but the diffraction peaks for sample B are slightly broadened due to smaller crystallite size.

The average crystallite size for both the samples was calculated using Scherrer formula [18]

$$L = \frac{0.89\lambda}{\beta \cos\theta}$$

where L is the crystallite size, λ is the X-ray wavelength, θ is the Bragg diffraction angle and β is the peak width at half width maximum (FWHM). The average crystallite size for samples A and B

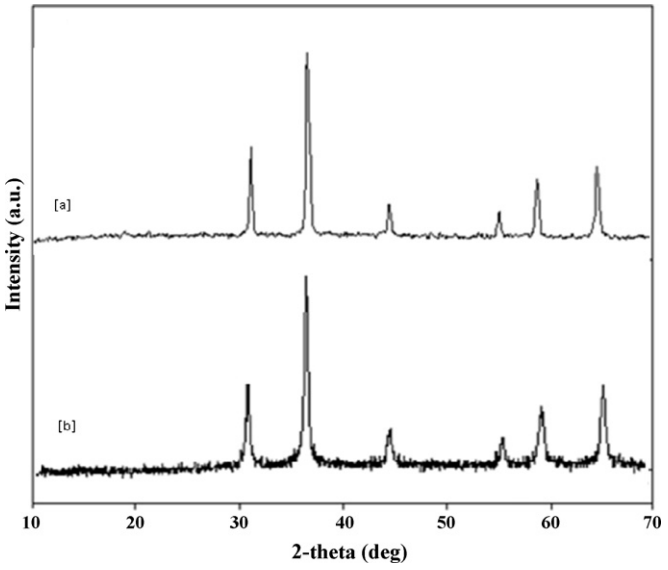

Fig. 1. XRD patterns of the nano copper aluminate samples: (a) sample A (prepared by sol–gel method); (b) sample B (prepared by modified sol–gel method).

Table 1
Crystallite size from the diffraction peak broadenings and activation energy calculated using Arrhenius equation for the nano $CuAl_2O_4$ spinel samples.

2θ (degree)	Crystallite size, L (nm)		Activation energy, E_a (eV)	
	Sample A	Sample B	Sample A	Sample B
31.18	28	27		
36.91	28	26		
44.90	33	28	0.23	0.21
55.73	32	32		
59.44	33	26		
65.45	26	24		

was found to be 30 nm and 27 nm respectively. It was notable that addition of ethylenediamine decreases the crystallite size (Table 1).

3.2. Electrical conductance studies

To assure the ohmic contact of the electrodes, the room temperature electrical conductance measurements of the nanocatalysts were carried out. The temperature dependence of electrical conductance carried out in the temperature range 393–573 K suggested that the current increased with an increase in temperature (T).

From the Arrhenius plot of $\ln(I/I_0)$ vs $1/T$ the activation energies were calculated from the linear portion of the plot (Fig. 2). The activation energy values for sample A (sol–gel method) and for sample B (modified sol–gel route) are 0.23 eV and 0.21 eV respectively. The lower activation energy value for sample B than that of sample A indicates that sample B requires comparatively a low energy required for producing the charge carriers. The study also confirms that both the samples are semiconductors.

The activation energy for electrical conduction in polycrystalline materials generally involves the combination of the energy required to raise the carriers from the dominant levels to their corresponding transport bands and the energy required to create the carriers from the dominant levels [19].

3.3. Thermoelectric power (TEP) measurements

The potential difference ΔV across the pelleted samples due to temperature difference ΔT for both the samples was measured. The cations on A-site as well as those on B-site contribute to the Seebeck coefficient and it shows similar n-type conduction, where electrons are the majority charge carriers (−ve) for both samples A and B. The absolute value of Seebeck coefficient for the copper aluminate samples prepared by sol–gel (sample A) was higher than the one prepared by modified sol–gel route (sample B). The plot of Seebeck coefficient for sample A and sample B is shown in Fig. 3.

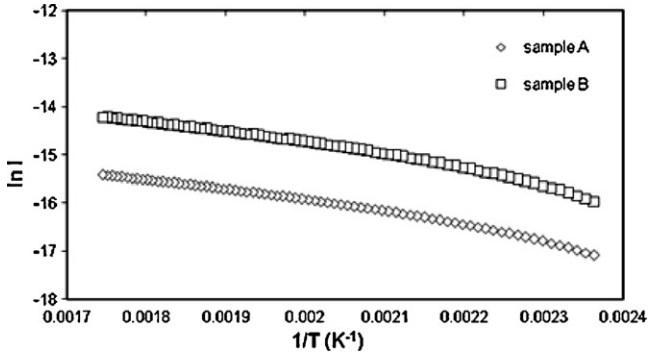

Fig. 2. Plot of $\ln(I/I_0)$ vs $1/T$ of copper aluminate samples: (a) sample A and (b) sample B.

3.4. Fourier transform infrared (FT-IR) analysis

The FT-IR spectra (Fig. 4a and b) of $CuAl_2O_4$ samples prepared by sol–gel method and modified sol–gel route exhibited a broad band near 3400 cm^{-1} due to —OH stretching vibration of free hydrogen bonded hydroxyl groups and a second typical absorption region at 1630 cm^{-1} assigned to the deformative vibration of water molecules, which is most probably due to water absorption by the samples during the compaction of the powder specimen with KBr [13]. The absorption peak of sample B (Fig. 4b) undergoes a red shift for H_2O molecule (from 3448 to 3435 cm^{-1} and from 1638 to 1633 cm^{-1}) and becomes weaker when compared with sample A (Fig. 4a), indicating the reduction in the degree of binding of H_2O on the surface of bigger crystallites due to the reason that they have less atoms/surface unit for the binding interaction with H_2O molecules. The metal oxygen stretching frequencies in the range of 500–900 cm^{-1} are associated with the vibrations of Al—O, Cu—O—Al bonds for sample A and sample B. Two sharp bands observed at 817 and 579 cm^{-1} are of copper aluminate spinels. These bands correspond to the AlO_6 units, which build up the $CuAl_2O_4$ spinel and indicate the formation of $CuAl_2O_4$ spinels [20]. However these bands are also found to be shifted in sample B that may be attributed to reduction in size of the nano grains which are IR active. For a nanosize grain, the atomic arrangements on the boundaries differ greatly from those of bulk crystals, both in co-ordination number and bond lengths, showing some extent of disorder [21]. Crystal symmetry is thus degraded in nanosize grains. The degradation in crystal symmetry results in the shifting of IR active mode [22].

3.5. N_2 adsorption/desorption isotherms

The nitrogen adsorption–desorption isotherm values at 77 K of the samples A and B are given in Table 2. Surface area parameters of the samples varied according to the preparation method. The copper aluminate sample prepared by sol–gel route possessed a surface area of 10.28 m^2/g, whereas for sample B, the BET surface area increased considerably to 41.83 m^2/g. The addition of ethylenediamine retards the growth of the bulk copper aluminate

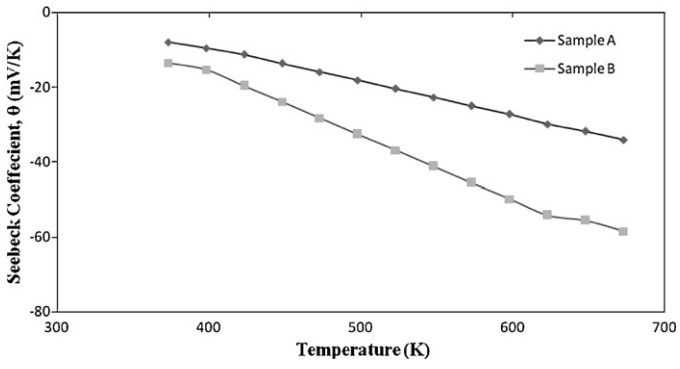

Fig. 3. Thermoelectric power (TEP) measurements of nano $CuAl_2O_4$ samples.

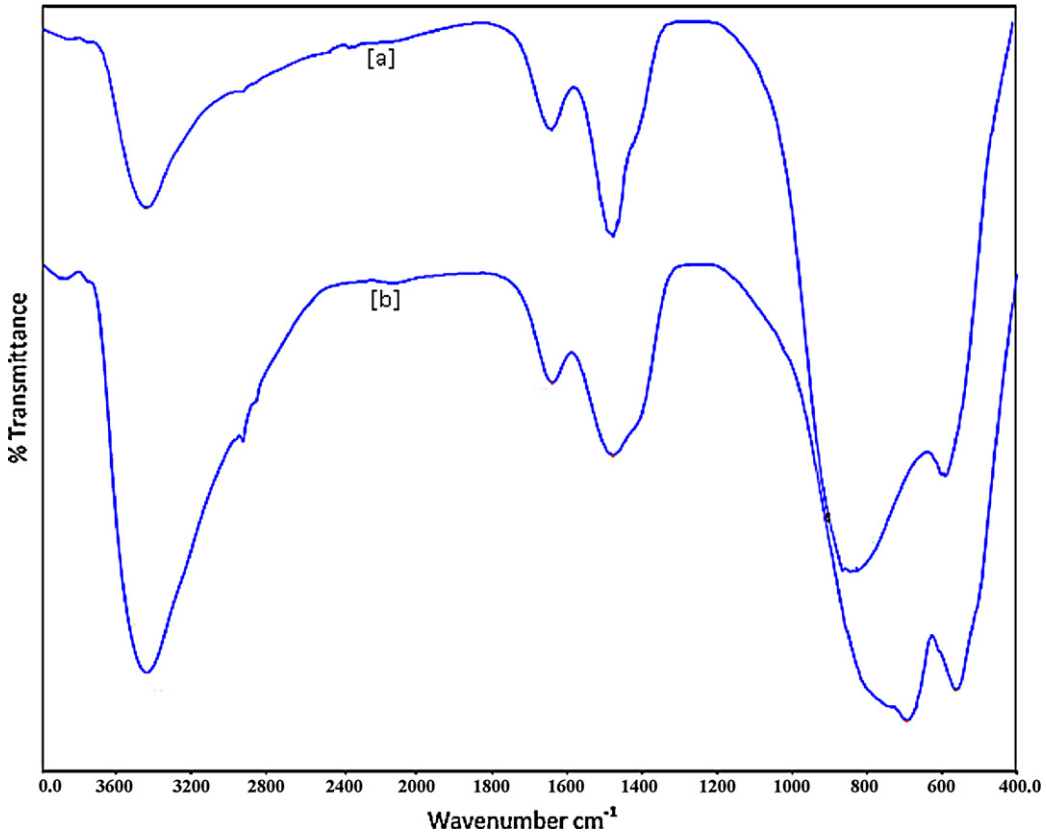

Fig. 4. Fourier transform infrared (FT-IR) spectra of copper aluminate samples: (a) sample A and (b) sample B.

Table 2
The surface area parameters of nano $CuAl_2O_4$ samples.

Surface area parameters	Sample A	Sample B
S_{BET} (m^2/g)	10.28	41.83
S_{mic} (m^2/g)	0	0
S_{meso} (m^2/g)	10.28	41.83
Total pore volume (cm^3/g)	0.1685	0.5722
Micropore volume (cm^3/g)	0	0
Mesopore volume (cm^3/g)	0.1209	0.5722
Average pore diameter (nm)	42.2	27.06

phase because of its property of strong coordination interaction with metal ions, leading to an increase in the surface area and enhancement in porosity. It is interesting to note that both the samples A and B are mesoporous materials (micropore surface area is zero) which is highly required in many industrial applications like in catalytic reactions. The average pore diameters of samples A and B were 42.24 and 27.02 nm, respectively. The average pore diameter of the samples is due to the formation of intergranular pores within the combination of metal oxides. The decrease in the average pore diameter for sample B can be attributed to the reduction in grain size, which is later confirmed by SEM studies.

3.6. Surface morphology, HR-TEM and elemental analysis (EDX)

The surface morphology of sample A and sample B was investigated by the scanning electron microscopy (SEM) images as shown in Fig. 5a and b. From the images it is observed that the sample B prepared by the modified sol–gel process is highly porous in nature with varying pore diameters (Fig. 5b) compared to sample A. The well organized pores from sample B might be due to the fact that the ethylenediamine added during the synthesis and further heat treatment temperature employed enabled a combustion assisted process. This creation of porosity in sample B leads to the increase

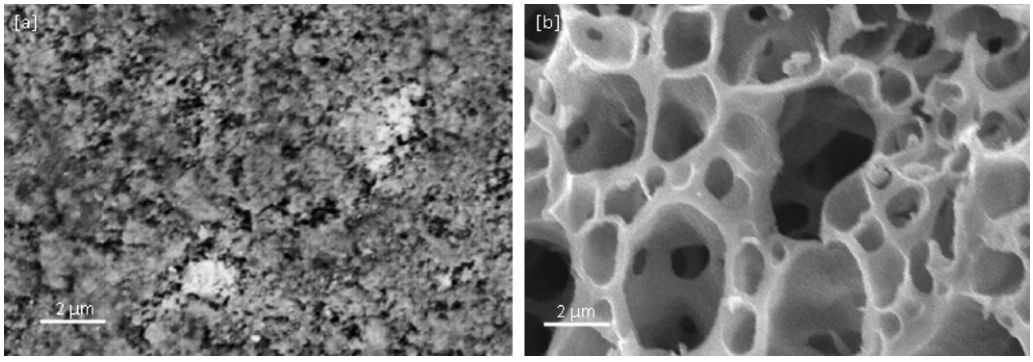

Fig. 5. SEM images of copper aluminate samples: (a) sample A and (b) sample B.

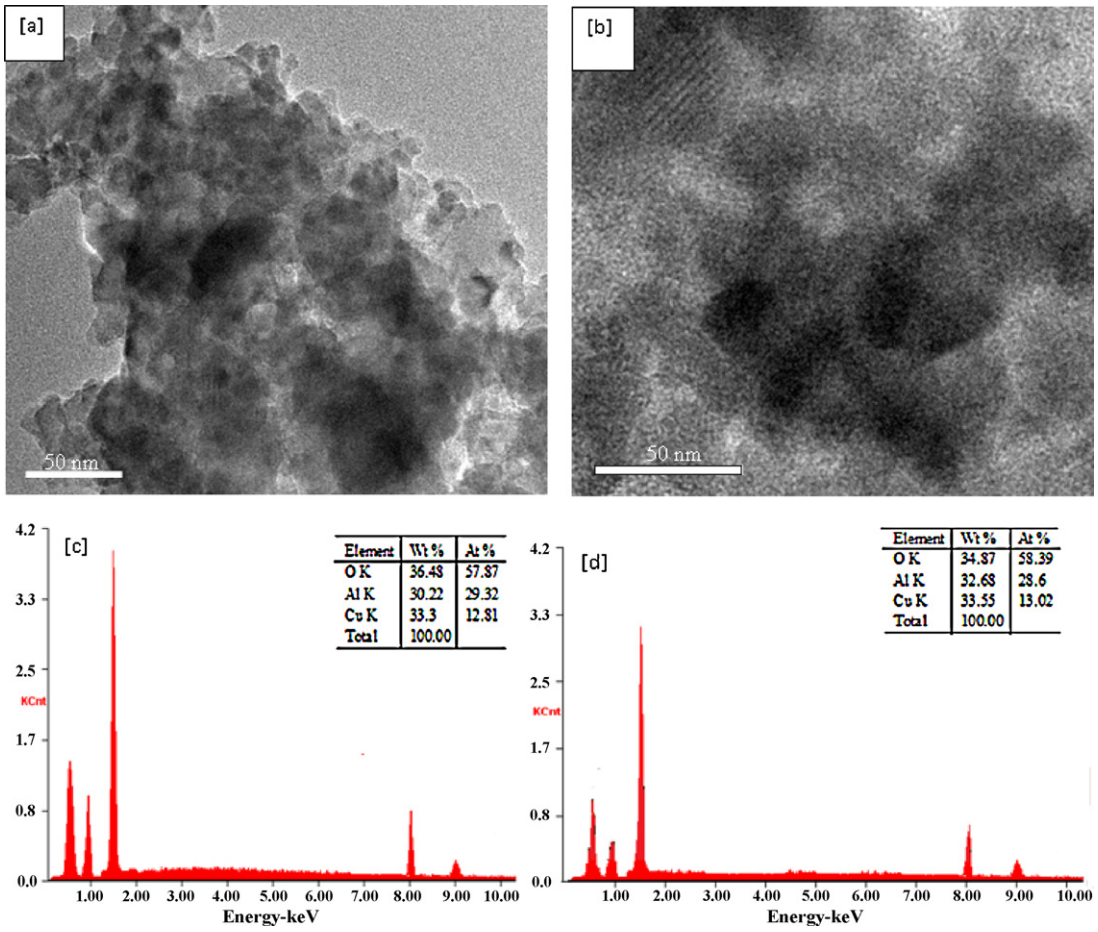

Fig. 6. HR-TEM images of copper aluminate samples: (a) sample A and (b) sample B. EDX spectrum of (c) sample A and (d) sample B.

in total BET surface area (41.83 m^2/g) while with sample A, BET surface area of 10.28 m^2/g was only achieved. Hence the SEM analysis indicates higher the porosity, higher the catalytic reactive sites.

The HR-TEM images for samples A and B are shown in Fig. 6a and b respectively. The high density of pores present in sample B can be easily recognized from the images of HR-TEM while the pores in sample A are difficult to locate leaving only the particles behind. Thus the image obtained from SEM and HR-TEM is an indicative that the modified sol–gel process adopted for sample B is one of the representative methods of preparing highly porous materials for catalytic applications.

The energy dispersive X-ray analysis shown in figure gives qualitatively the presence of Cu, Al and O without any other characteristic peaks in $CuAl_2O_4$ spinels irrespective of the method of preparation. It is also definitive evidence to suggest that the samples A and B do not contain any other element and are indeed free from other impurities.

3.7. UV–visible diffuse reflectance (UV–vis-DRS) spectral studies

The optical properties of the copper aluminate samples A and B were measured by UV–visible DRS spectra [23]. The band gap of these samples was estimated from the fundamental absorption edge or coefficient. The optical gap was calculated using the Tauc relation by plotting $(\alpha h\nu)^2$ against $h\nu$ where α and $h\nu$ denote the absorption coefficient and photon energy respectively and by extrapolating the curve to the photon energy axis. The absorption coefficient is given by $\alpha = 2.303(A_b/t)$, where A_b is absorbance and t is the thickness of the sample [24]. The Tauc's plot is shown in Fig. 7 and the band gap for the sample A and sample B is 1.62 eV and 1.70 eV respectively. The results shows that for the sample B prepared by modified sol–gel process, the absorption band edge slightly shifts towards the blue region indicating a very weak quantum size effect to that of the sample A prepared by sol–gel method. Hence there is a small increase in the optical band energy value for sample B compared to that of sample A. This is in good agreement with the results of XRD analysis. The results from XRD suggested the crystallite size for sample B is slightly lower than that of sample A. Thus the shift in the fundamental absorption edge towards

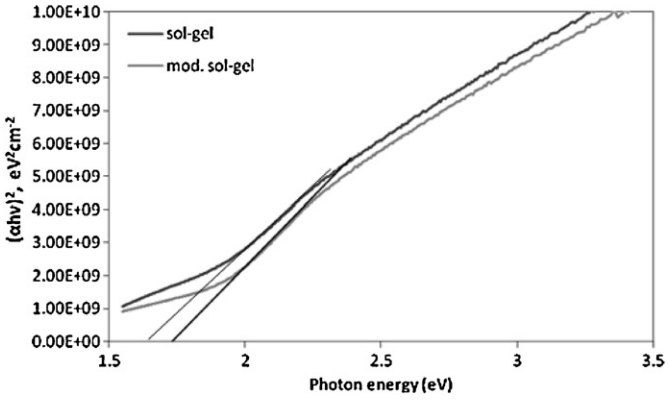

Fig. 7. Diffuse reflectance spectra (DRS) of the $CuAl_2O_4$ samples: (a) sample A and (b) sample B.

lower wavelength for sample B may be attributed to a decrease in the crystallite size.

3.8. The mechanism of the formation of copper aluminate

The chemical reactions taking place between citric acid, ethylenediamine and the metal nitrates are given in Eq. (1).

$$9Cu(NO_3)_2 + 18Al(NO_3)_3 + 20C_6H_8O_7 \xrightarrow{C_2H_8N_2,\ \Delta} 9CuAl_2O_4 + 120CO_2 + 36N_2 + 80H_2O \quad (1)$$

The addition of citric acid with ionic solutions of copper and aluminum leads to the formation of complexation or chelation between these metal ions and the chelating agent i.e. citric acid. The complexation reaction promotes the compositional homogeneity of the metal salts in the solution during the intermediate process and thereby leads to the formation of three dimensional structures. The addition of ethylenediamine in the present study is to promote the combustion process. Based on the propellant chemistry and thermodynamic calculations CO_2, N_2, and H_2O are the most stable products of the combustion synthesis reaction [25]. The ethylenediamine molecule in the present synthesis procedure plays a dual role in enhancing further compositional homogeneity. As compositional homogeneity is one of the prerequisites in the catalyst preparation, ethylenediamine favors this homogeneity by avoiding the precipitation of the individual or selective components. On the other hand, ethylenediamine plays as an excellent fuel for the combustion to take place as it is easily oxidizable by nitrate ions.

Thus the combined effect of the roles played by citric acid and ethylenediamine in homogeneous mixing of the reactants at the atomic or molecular scale levels and combustion reaction taking place at an extremely faster rate respectively results in the nucleation process for the growth of nano sized copper aluminate sample.

3.9. Catalytic oxidation of benzyl alcohol using samples A and B

The catalytic oxidation of benzyl alcohol was employed as a model reaction to investigate the performance of copper aluminate catalysts (samples A and B). A comparison of the nano copper aluminate samples prepared by sol–gel (sample A) and modified sol–gel route (sample B) with respect to their surface properties and benzyl alcohol to benzaldehyde oxidation activity (Table 3) provides the following information. Catalytic studies showed that the preparation technique has a strong influence on both the conversion and product selectivity. The conversion of benzyl alcohol reaches a maximum, for sample B (100%) whereas for sample A the conversion was only 76%. The highest activity of the sample B prepared by modified sol–gel route is due to the highest surface area, smaller crystallite size and highest porosity.

The rate of oxidation of benzyl alcohol can be normalized by the specific area of the catalyst using the pseudo first order rate model proposed by Johnson et al. [26].

$$\ln\left(\frac{C_t}{C_0}\right) = -k_{SA}\rho_A(t) = -k_{obs}(t)$$

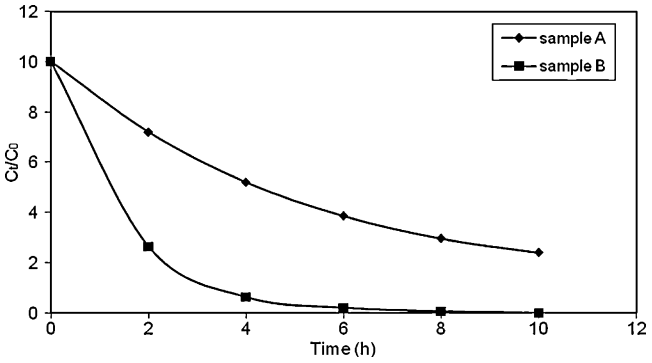

Fig. 8. Oxidation of benzyl alcohol at various time intervals for copper aluminate samples.

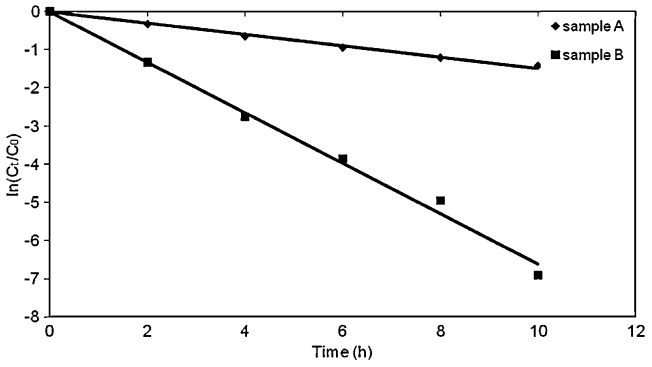

Fig. 9. Pseudo first order rate kinetics of benzyl alcohol oxidation for copper aluminate samples.

where C_t is the benzyl alcohol concentration at a given time, t (in mM), C_0 is the initial benzyl alcohol concentration (in mM), k_{SA} is the surface normalized reaction rate constant ($h^{-1}\,m^{-2}\,L$), ρ_A is the specific surface area concentration of the catalyst in the solution ($m^2\,L^{-1}$). The surface normalized reaction rate or the specific reaction rate k_{SA} is equal to the observed rate constant (k_{obs}) divided by the specific surface area concentration ρ_A. The k_{obs} values were calculated from the linearized plot of the pseudo first order rate model and later on was used for the calculation of specific reaction constant (k_{SA}). From Figs. 8 and 9 it is seen that the oxidation of benzyl alcohol to benzaldehyde follows the pseudo first order rate kinetics as observed from the regression analysis that is greater than 0.98. The surface normalized rate constant k_{SA} obtained for the oxidation of benzyl alcohol using the samples A and B was $1.60 \times 10^{-4}\,h^{-1}\,m^{-2}\,L$ and $1.74 \times 10^{-4}\,h^{-1}\,m^{-2}\,L$ respectively. A notable higher value of k_{SA} in sample B shall be attributed to the increase in surface active sites that was easily accessible for the reactants and thus favoring the oxidation of benzyl alcohol to benzaldehyde.

It may be noted that not only the conversion but also the benzaldehyde selectivity was higher for the sample B prepared by modified sol–gel route (Table 3).

Table 3
Properties of copper aluminate samples A and B and their activity in benzyl alcohol oxidation.

Catalyst	Surface area (m^2/g)	Conversion (%) of benzyl alcohol	Selectivity (%) for benzaldehyde[a]	k_{obs} (h^{-1})	k_{SA} ($m^{-2}\,h^{-1}\,L$)
Sample A	10.28	76	85	0.15	1.60×10^{-4}
Sample B	41.83	99.9	99.9	0.662	1.74×10^{-4}

Reaction conditions: catalyst, 1 g; acetonitrile, 10 mmol; H_2O_2, 10 mmol; temperature, 80 °C; time, 10 h.

[a] The other product obtained was benzoic acid.

Table 4
Effect of solvent on the yield and selectivity percentage for the oxidation of benzyl alcohols by sample B prepared by modified sol–gel route.

Solvent	Temp. (°C)	Conversion (%)	Selectivity (%)[a]
Acetonitrile	80	100	100
Hexane	80	87.8	95
Chlorobenzene	80	2.1	90

Reaction conditions: catalyst, 1 g; solvent, 10 mmol; H_2O_2, 10 mmol; time, 10 h.
[a] The other product obtained was benzoic acid.

Since the sample B was found to be the most active and selective one for the benzyl alcohol oxidation reaction, we investigated the influence of solvents on the oxidation of benzyl alcohol.

The effect of solvent on the percentage yield and selectivity percentage is given in Table 4. From the results, it is found that acetonitrile gives the highest selectivity, followed by n-hexane and chlorobenzene. In case of acetonitrile, it activates H_2O_2 by forming a perhydroxyl anion (OOH^-) that nucleophilically attacks the nitrile to generate a peroxycarboximidic acid intermediate, which is a good oxygen transfer agent. Both organic substrate and the aqueous H_2O_2 dissolve in acetonitrile forming a uniform solution [27]. In case of n-hexane appreciable yields are observed next to acetonitrile owing to the competition from hydrogen transfer with the solvent. In case of chlorobenzene, it is less, as it adsorbs strongly on the catalyst surface and competes with the adsorption of benzyl alcohol.

4. Conclusions

In this study, nano copper aluminate spinel was prepared by sol–gel and modified sol–gel route. The effect of the preparation method on the structural, electrical, optical properties and catalytic activity for selective oxidation of benzyl alcohol was investigated. Characterization results showed that the highest surface area, smaller crystallite size, low activation energy (E_a) and more porosity were obtained from the sample prepared by modified sol–gel route. From the results, it was found that the nano copper aluminate prepared by modified sol–gel route (sample B) was found to be highly active towards the selective oxidation of benzyl alcohol to benzaldehyde at low temperature with very high yield because of more number of active sites and lower activation energy due to the addition of ethylenediamine. Hence the addition of ethylenediamine during the preparation procedure enhances the catalytic properties of copper aluminate.

Acknowledgements

The authors duly acknowledge the financial support rendered by the Department of Science and Technology (DST), India, through the Young Scientist Project Scheme (DST-Ref. No. SR/FTP/CS-117/2007).

References

[1] A. Troia, M. Pavese, F. Geobaldo, Ultrason. Sonochem. 16 (2009) 136.
[2] R. Katamreddy, R. Inman, G. Jursich, A. Soulet, C. Takoudis, Acta Mater. 56 (2008) 710.
[3] W.S. Hong, L.C.D. Jonghe, J. Am. Ceram. Soc. 78 (1995) 3217.
[4] Z.Q. Tian, H.T. Yu, Z.L. Wang, Mater. Chem. Phys. 106 (2007) 126.
[5] S.L. Wu, S.F. Zhang, J.Z. Yang, Mater. Chem. Phys. 102 (2007) 80.
[6] L.T. Chen, C.S. Hwang, I.G. Chen, S.J. Chang, J. Alloys Compd. 426 (2006) 395.
[7] D. Mishra, S. Anand, R.K. Panda, R.P. Das, Mater. Chem. Phys. 82 (2003) 892.
[8] S. Cizauskaite, V. Reichlova, G. Nenartaviciene, A. Beganskiene, J. Pinkas, A. Kareiva, Mater. Chem. Phys. 102 (2007) 105.
[9] Pechini MP, US 3330697, 1967.
[10] W. Lv, B. Liu, Q. Qiu, F. Wang, Z. Luo, P. Zhang, S. Wei, J. Alloys Compd. 479 (2009) 480.
[11] W. Lv, Z. Luo, H. Yang, B. Liu, W. Weng, J. Liu, Ultrason. Sonochem. 17 (2010) 344.
[12] M. Salavati Niassari, F. Davar, M. Farhadi, J. Sol–Gel Sci. Technol. 51 (2009) 48.
[13] J.J. Vijaya, L.J. Kennedy, G. Sekaran, K.S. Nagaraja, Mater. Res. Bull. 43 (2008) 473.
[14] J.J. Vijaya, L.J. Kennedy, G. Sekaran, K.S. Nagaraja, M. Bayhan, M.A. William, Sens. Actuators B 134 (2008) 604.
[15] S. Brunauer, P.H. Emmett, E.J. Teller, J. Am. Chem. Soc. 60 (1938) 309.
[16] S.J. Gregg, K.S.W. Sing, Adsorption, Surface Area and Porosity, Academic Press, London, 1982, p. 100.
[17] D.R. Patil, L.A. Patil, Sens. Actuators B 120 (2006) 316.
[18] R. Bouberki, Z. Beji, K. Elkabous, F. Herbst, G. Viau, S. Ammar, F. Fievet, J.H.V. Bardeleben, A. Mauger, Chem. Mater. 21 (2009) 843.
[19] R. Sundaram, E.S. Raj, K.S. Nagaraja, Mater. Res. Bull. 39 (2004) 1737.
[20] H. Liu, Z. Wang, H. Hu, Y. Liang, M.J. Wang, Solid State Chem. 182 (2009) 1726.
[21] J. Lu, H. Yang, B. Liu, G. Zou, Scripta Mater. Res. Bull. 34 (1999) 2109.
[22] J. Mathew, S. Kurian, M. Thomas, K.C. George, Indian J. Pure Appl. Phys. 42 (2004) 121.
[23] J. Yanyan, L. Jinggang, S. Xiaotao, N. Guiling, W. Chengyu, G. Xiumei, J. Sol–Gel Sci. Technol. 42 (2007) 41–45.
[24] A. Azam, A. Jawad, S. Arham Ahmed, M. Chaman, A.H. Naqvi, J. Alloys Compd. 426 (2006) 395.
[25] Z. Shao, W. Zhou, Z. Zhu, Prog. Mater. Sci. 57 (2012) 804.
[26] T.L. Johnson, M.M. Sherer, P.G. Tratnyek, Environ. Sci. Technol. 30 (1996) 2634.
[27] U.R. Pillai, E. Sahle-Demessie, Appl. Catal. A: Gen. 276 (2004) 139.